Heliyon 10 (2024) e26307

Contents lists available at ScienceDirect

Heliyon

journal homepage: www.cell.com/heliyon

Research article

Noninvasive wearable sensor for the continuous monitoring of human sound and movement signals in real-time

Eun Ae Choi [a,b], Jeong Chan Lee [d], Mi Yu [f], Hyo Sung Kwak [g,h], Bishnu Kumar Shrestha [c,***], Chan Hee Park [a,c,d,e,**], Cheol Sang Kim [c,d,e,*]

[a] Innovative Mechanobio Active Materials Based Medical Device Demonstration Center, Jeonbuk National University, Jeonju, Republic of Korea
[b] Interventional Mechano-Biotechnology Convergence Research Center, Jeonbuk National University, Jeonju, Republic of Korea
[c] Department of Bionanosystem Engineering, Graduate School, Jeonbuk National University, Jeonju, Republic of Korea
[d] Department of Bionanotechnology and Bioconvergence Engineering, Graduate School, Jeonbuk National University, Jeonju, Republic of Korea
[e] Department of Mechanical Design Engineering, Graduate School, Jeonbuk National University, Jeonju, Republic of Korea
[f] Division of Biomedical Engineering, College of Engineering, Jeonbuk National University Republic of Korea
[g] Research Institute of Clinical Medicine of Jeonbuk National University Biomedical Research Institute of Jeonbuk National University Hospital Republic of Korea
[h] Department of Radiology and Research Institute of Clinical Medicine of Jeonbuk National University Biomedical Research Institute of Jeonbuk National University Hospital Republic of Korea

ARTICLE INFO

Keywords:
Electrospinning
Bio-sensor
Peizo-electric
Polyaniline

ABSTRACT

Recently, with the development of non-invasive human health monitoring technology including wearable devices, a flexible sensor that monitors 'human sound and movement signals' such as human voice and muscle movement is attracting attention. In this experiment, electrospun nanofibers were mixed with highly conductive nanoparticles and coated with polyaniline to detect the patient's electrical signals. Due to the high piezoelectric effect, nanofiber-based sensors do not require charging through a separate battery, so they can be used as self-powered devices. In addition, the LCR meter test confirmed that the sensor has a high capacitance due to its high conductivity and high sensitivity to electrical signals. The sensor produced in this study can visually estimate the electrical signal of the actual human body through real-time comparison with electromyography (EMG) measuring equipment, and it was confirmed that the error is small. This sensor is expected to be widely used in the medical field, from simple sound and movement signals to disease monitoring.

1. Introduction

Recently, a sensor that monitors sound and movement signals, such as the patient's voice, vibration, and muscle movement, has attracted attention [1–4]. In the case of the existing system, since the patient is admitted to the hospital and is diagnosed, there is a problem of cost, or of not being able to receive real-time support in daily life. Therefore, there is a need for a sensor that can diagnose

* Corresponding author. Department of Bionanosystem Engineering, Graduate School, Jeonbuk National University, Jeonju, Republic of Korea.
** Corresponding author. Innovative Mechanobio Active Materials Based Medical Device Demonstration Center, Jeonbuk National University, Jeonju, Republic of Korea.
*** Corresponding author.
E-mail addresses: bishnuaampipal@hotmail.com (B.K. Shrestha), biochan@jbnu.ac.kr (C.H. Park), chskim@jbnu.ac.kr (C.S. Kim).

https://doi.org/10.1016/j.heliyon.2024.e26307
Received 27 July 2023; Received in revised form 26 November 2023; Accepted 9 February 2024
Available online 10 February 2024

the patient's condition in everyday life, rather than in a hospital [5].

According to previous research, the sensor being studied recently can detect changes in electrical properties such as resistance or capacitance to signals and obtain sound and movement signals. High accuracy [6] and long service life are the most important characteristics of electronic devices such as sensors [7–9]. In addition, since the sensor is attached to the body to detect the patient's sound and movement signals, high elongation, and mechanical strength are required. To develop such a high-sensitivity sensor, a nanofiber structure of polymers and nanoparticles with high piezoelectric performance and conductivity is essential, so that the intrinsic properties of the materials can work effectively [10,11].

Electrospinning is a representative technology for the manufacture of nanofibers and structures, and extensive research is being conducted in the field of filters and medicine, and in the field of electronic devices, such as batteries, heat dissipation, and electromagnetic wave shielding [12]. Polymers are generally used as the main material for electrospinning because of their lightweight, processability, and flexibility. We used Polyvinylidene fluoride (PVDF), which shows high conductivity and piezoelectric effect, and used Polyurethane (PU) to increase mechanical strength to fabricate the sensor. In addition, we add Al_2O_3 and coat polyaniline to improve conductivity and sensitivity.

In this study, a body-worn sensor with high piezoelectric performance and sensitivity was fabricated using electrospinning technology. We measured human sound and movement signals with the developed sensor and conducted comparative experiments with commercially available EMG test equipment.

The sensor produced in this paper has high accuracy and piezoelectric performance, so it does not require an unnecessary charging device, and it is expected that it can easily detect the patient's health signal in daily life by applying it to a wearable system, such as a smartwatch.

2. Materials and methods

2.1. Materials

Aluminum oxide (Al_2O_3; CAS Number:1344-28-1) and Polyvinylidene fluoride (PVDF) were purchased from Sigma–Aldrich S. Korea. Polyurethane (PU) was purchased from Estane® Skythane® (X595A-11, Lubrizol Advanced Materials, Inc., USA). Aniline ($C_6H_5NH_2$), Ammonium persulfate, N,N- Dimethylformamide (DMF), Acetone, and Sulfuric acid were purchased from Samchun, S. Korea. PC12 cell (fibroblast, Cell Line Bank, S. Korea), DMEM, Trypsin (Gibco), Cell Counting Kit (CCK−8, Dojindo, South Korea), and Live/Dead (L3224, Thermofisher) were used for biocompatibility Test. All the reagents were of analytical grade, and were used without further purification.

2.2. Electrospinning process

The Al_2O_3 nanoparticles were dispersed in a 1:1 ratio of DMF and Acetone for several hours. Then, 4, 8 wt% of PU and 10 wt% PVDF were added to the Al_2O_3 dispersion and then stirred in an oil bath at 48 °C for 12 h to prepare a solution. The solutions placed in a 12 mL syringe were extruded through a 21-gauge needle using a syringe pump. The distance between each needle and the collector was 15 cm. Electrospinning was performed at a high DC voltage of 15 kV. The feed rate of solution was set at 1 mL/h. Electrospinning was performed for 4 h. After electrospinning, the material was dried in a hood for at least one day to remove residual solvent.

2.3. Polyaniline coating process

Sulfuric acid and aniline were added to DI water to make 0.1 M H_2SO_4 0.1 M aniline solution. Ammonium persulfate was added to DI water to make a 0.1 M ammonium persulfate solution. The electrospun nanofibrous membrane was immersed in 0.1 M H_2SO_4 0.1 M aniline solution for 1 day. An ammonium persulfate solution at a ratio of 3:1 to 0.1 M H_2SO_4 0.1 M aniline solution was slowly dropped onto the nanofibrous membrane using a separatory funnel. After reacting to form a polyaniline coating for 1 day, it was washed with DI water to remove the residual solvent of the coated nanofiber membrane. After that, it was dried at room temperature for more than one day.

2.4. Physical characterizations

The surface morphology of fibrous membrane was characterized by Field emission scanning electron microscopy (FE-SEM, Carl Zeiss, SUPRA40VP, Germany), equipped with energy dispersive electron microscopy. Multi-Purpose High-Performance X-ray Diffractometer (MPD-XRD, PANalytical, X'PERT-PRO Powder, Netherlands) was performed to check whether Al_2O_3 was present in the fiber. Fourier Transform infrared spectrometer was used to analyze the piezo effect increase by comparing the peaks of β phase and α phase. A hybrid- X-ray photoelectron spectrometer system (Hybrid XPS system) was performed the presence of Al_2O_3 was confirmed for the Binding Energy peak of Al_2O_3 in the fiber. Thermal Analyzer (TGA, WATERS, DSC Q20) was performed under several 5 °C/min at 50 °C–900 °C in a nitrogen atmosphere. Universal Testing Machine (UTM, MTDI Inc., UT-020E, South Korea) was performed to compare the mechanical performance of the sensor. A 1 N load cell was used and the displacement control was set to have a speed of 20 mm/min. At least three dog-bone-shaped samples were made and evaluated for each group.

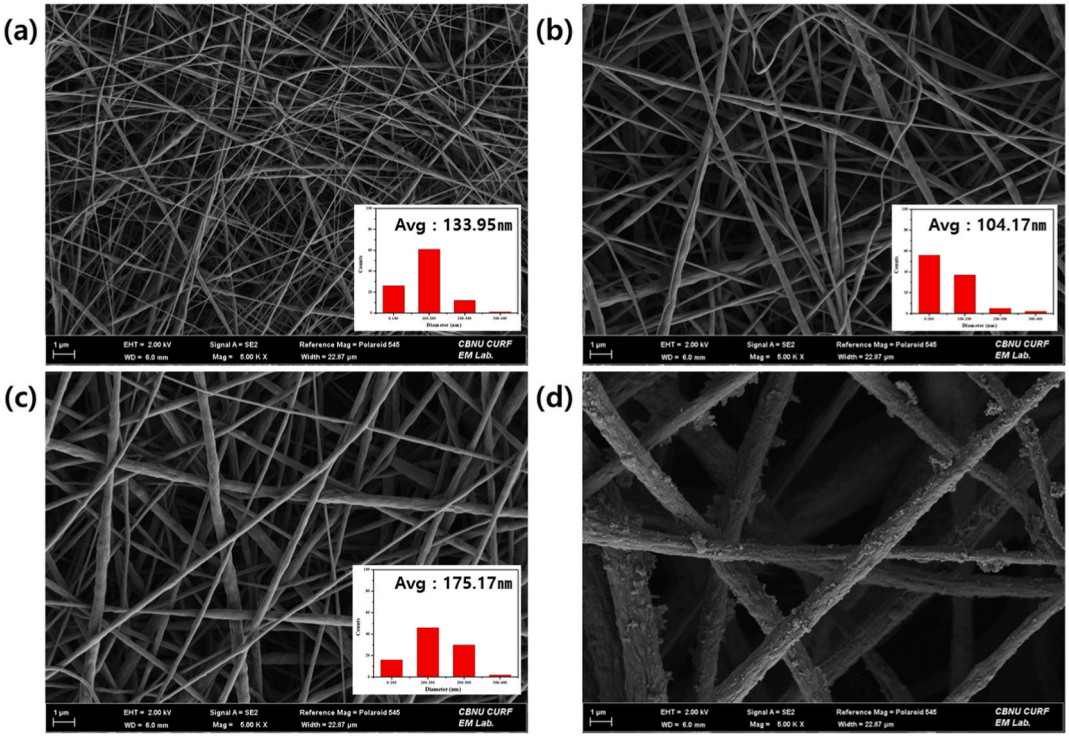

Fig. 1. FE−SEM images of electrospun nanofiber (a) PU, (b) PVDF, (c) PU/PVDF/Al_2O_3, (d) PU/PVDF/Al_2O_3/PA.

2.5. Electrochemical studies

The charge transfer resistance (Rct) behavior of the PU and PU/PVDF/Al_2O_3 and PU/PVDF/Al_2O_3/PA substrates was evaluated using a four-point probe system (MCJ1 conductivity Test Jig (WonATech Co. Ltd., Seoul), on the basis of electrochemical impedance spectroscopy (EIS) at conditions of zero bias potential, with an amplitude of 10 mV and a frequency range of (100 kHz–0.1 Hz). In addition, we measured the sheet resistance properties to determine the electrical conductivity of the substrates using a Four-Point Probe system (CMT-SR1000 N, AiT Co., Ltd., Advanced Instrument Technology, South Korea).

2.6. Piezoelectric characterization

The electrospun nanofiber sample is cut into a size of 20 mm × 20 mm. Apply copper tape and OHP film to the sample, and connect by soldering the wires. At this time, the sample area should be larger than the copper tape and smaller than the OHP film. When the sample is finished, it is held in the center of the insulating plate under the bar, which applies pressure from the piezoelectric shaker (Camtic, Korea). Using the oscilloscope's scope (Agilent Technologies, DSO1012A), connect it according to the (+) and directions of the sample. Apply pressure of 2,4,6,8 Hz frequency using the piezo program. When frequency pressure is applied, use an oscilloscope to check the sensor's piezo voltage. For accuracy, save the data after at least 3 min after the machine is started. In addition, in order to obtain accurate data, it was determined that the data could be used when similar values were obtained through two or more piezo tests.

2.7. LCR METER test

Samples are prepared in the same method as in the piezo experiment. Unlike piezo machines, in the case of an LCR meter test that measures capacitance, the larger the area of the sample, the larger the capacitance. This is because the larger the area, the more charge is generated for a given voltage. So, it is important to make all samples the same size. In addition, when measuring the capacitance, data errors may occur due to static electricity, so be sure to insulate. In this way, an OHP film was attached to the sample attached with copper tape. In the case of applying a frequency pressure, it is fixed to the center of the insulating plate under the bar of the piezo machine in the same way as the piezo measurement. Connect the sample line to the LCR meter scope. Apply a pressure of 0.1,0.5 Hz frequency using the piezo program. The reason the size of the frequency is different from the piezo machine is that the LCR meter needs time to be charged and discharged differently from the piezo machine, so it cannot be measured at too large a frequency. When applying frequency pressure, measure the capacitance using the LCR meter program.

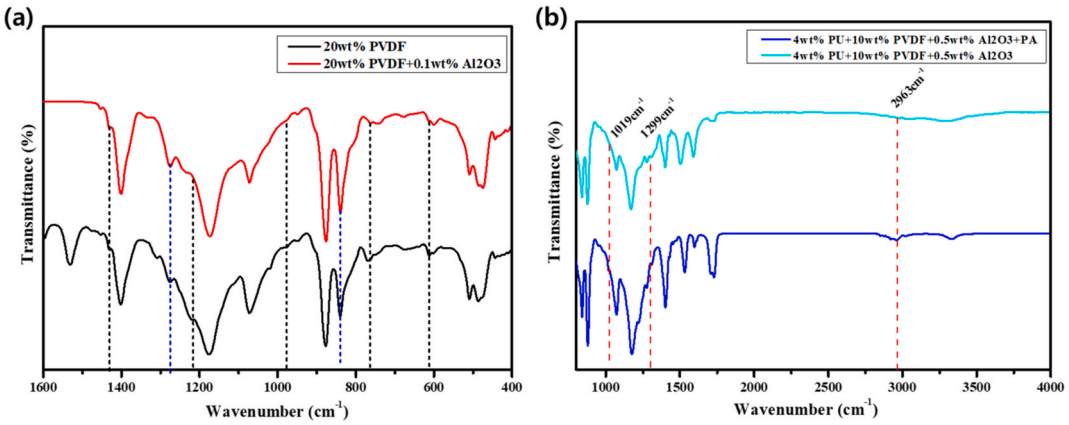

Fig. 2. Fourier Transform Infrared Spectrometer. (a) Comparison of α-phase and β-phase of PVDF and PVDF/Al_2O_3 (b) Comparison of PU/PVDF/Al_2O_3 and PU/PVDF/Al_2O_3/PA.

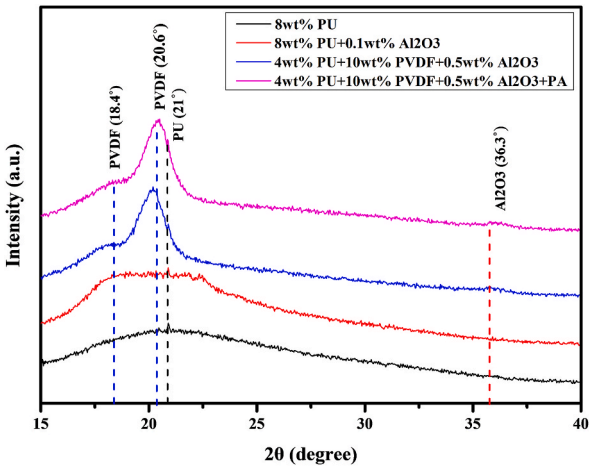

Fig. 3. X-ray diffractometer of PU, PU/Al_2O_3, PU/PVDF/Al_2O_3, PU/PVDF/Al_2O_3/PA.

2.8. In vitro biocompatibility test

PC12 (from Cell Line Bank, Korea) was cultured on DMEM (Gibco Thermo Fisher Scientific). The cultured cells were passaged three times by trypsinization, before seeding. The different scaffolds with dimensions of (1.2 cm × 1.2 cm) were fixed into the 96-well plates and sterilized under UV overnight, then washed with 96 % ethanol, followed by washing with PBS. The samples were again pretreated with a complete medium for 3 h, and seeded at a density of 1.5 × 104 cells/well on each electrospun mat by pipetting onto the center, before placement in the incubator for (1, 3, and 5) days. The cells were nourished with fresh medium every second day. The adhesion, proliferation, and viability of the cells on the scaffolds were examined by the cell counting kit-8 (CCK-8). The CCK-8 test solution was added to each well plate, and incubated for 2 h at 37 °C. The optical density was measured at 450 nm wavelength using a microplate reader (Tecan, Austria).

3. Results

3.1. Morphological characterization

The surface of the electrospun membrane was observed using FE−SEM (Fig. 1). As seen in each fiber image, it was confirmed that all sample groups did not have a bead shape, and thin fibers were formed uniformly in the diameter of the fibers as a whole (Fig. 1 (a–c)). In addition, observation of the fibers subjected to the polyaniline coating confirmed that the layer was made uniformly on the surface and inside (Fig. 1(d)).

FT-IR and XRD analyzes were performed on samples produced under various conditions to evaluate the effect of PVDF, Al_2O_3 addition, and PA coating on the phase and crystal structure of electrospun fibers. First, FT-IR analysis was performed to support that

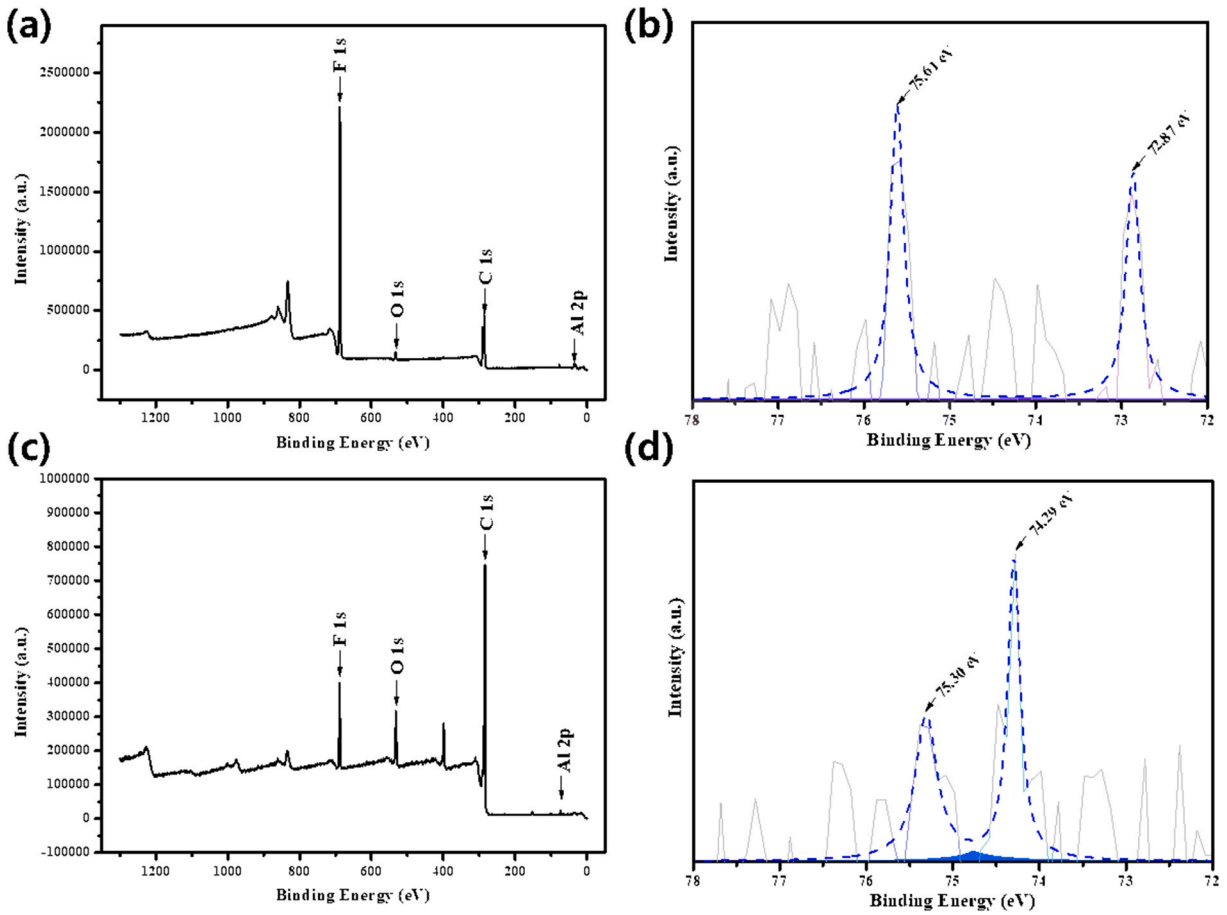

Fig. 4. Hybrid- X-ray photoelectron spectrometer system. (a) and (b) PU/PVDF/Al_2O_3, (c) and (d) PU/PVDF/Al_2O_3/PA.

the piezoelectric effect was increased with the loading of Al_2O_3 in the nanofibers. Prepared 20 wt% PVDF and 4 wt% PU+10 wt% PVDF+0.5 wt% Al_2O_3 fibers were compared. The β-phase induces a change in dipole moment through zigzag H-bonds stretching. The piezoelectric effect is higher when it has a regular shape like β-phase, which is a crystalline area, rather than α, which is an amorphous area. The β-phase is polar and shows ferroelectric and piezoelectric properties. So, if the β-phase peak is large, it can support a high piezo effect. We can find the FT-IR data of the samples in Fig. 2. In Fig. 2(a) we can check that the α phase such as 1423, 1209, 975, 763, and 614 cm^{-1} shows a smaller peak in the fiber mixed with Al_2O_3 than in the general PVDF. In the β-phase such as 1275, and 841 cm^{-1}, it can be seen that the sample mixed with Al_2O_3 shows a larger β-phase. So, it was confirmed that when Al_2O_3 was mixed, a higher piezoelectric effect was observed. In Fig. 2(b), we can check e the coating of polyaniline on the fiber. The peak at 1299 cm^{-1} corresponds to the π-electron delocalization induced in the protonation of the polymer. The broad peak at 2961 cm^{-1} shows aromatic C–H stretching.

Fig. 3 shows the XRD pattern of the materials. Where, 8 wt% PU and 8 wt% PU+0.1 wt% Al_2O_3 and 4 wt% PU+10 wt% PVDF+0.5 wt% Al_2O_3 and 4 wt% PU+10 wt% PVDF+0.5 wt% Al_2O_3+Polyaniline Coating samples were compared. In 8 wt% PU, only the peak of the PU was observed at 21°. Since the Al_2O_3 nanoparticles are not only small in size and their content is too small, the peak of Al_2O_3 could not be found in 8 wt% PU+0.1 wt% Al_2O_3, and only the peak of PU could be found at 21°. In the 4 wt% PU+10 wt% PVDF+0.5 wt% Al_2O_3 sample, because of the increased amount of Al_2O_3, small peaks of Al_2O_3 were found at 36.3°, and peaks of PVDF were also found at 18.4° and 20.6°. It's really weak, but at 21° we could also find the peak of PU. In the polyaniline-coated sample of 4 wt% PU+10 wt% PVDF+0.5 wt% Al_2O_3, the peak of PVDF at 18.4° and 20.6° and the peak of PU at small 21° were found. As before, a small peak of Al_2O_3 was found at 36.3° due to the increased Al_2O_3 content. However, more analysis was conducted to find Al_2O_3 for accurate confirmation.

To further confirm the presence of Al_2O_3 in the nanofibers, XPS analysis of prepared nanofiber mats was also performed. The presence of Al_2O_3 is clearly visible in the 4 wt% PU+10 wt% PVDF+0.5 wt% Al_2O_3 sample (Fig. 4(a)) and 4 wt% PU+10 wt% PVDF+0.5 wt% Al_2O_3 + Polyaniline sample (Fig. 4(c)). In the case of 4 wt% PU+10 wt% PVDF+0.5 wt% Al_2O_3, peaks were found at Binding energies of 72.87 eV and 75.61 eV (Fig. 4(b)). In the case of 72.87 eV, it is the binding energy of the Al metal state. In the case of 75.61 eV, it is the binding energy of Al oxide on the Al foil state. These peaks indicate that the fiber has three Al states such as an Al metal state and an Al oxide on the Al foil state. In the case of the Al metal state, it is the state when Al reacts with oxygen (Al–O state). Al

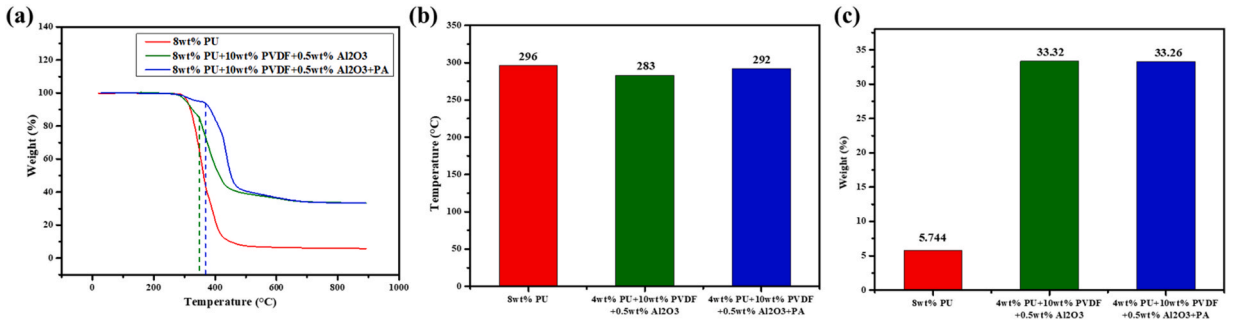

Fig. 5. Thermogravimetric Analysis. (a) PU and PU/PVDF/Al_2O_3 and PU/PVDF/Al_2O_3+PA. (b) Comparison of Temperature at which the weight begins to decrease. (c) Comparison of the remaining weight.

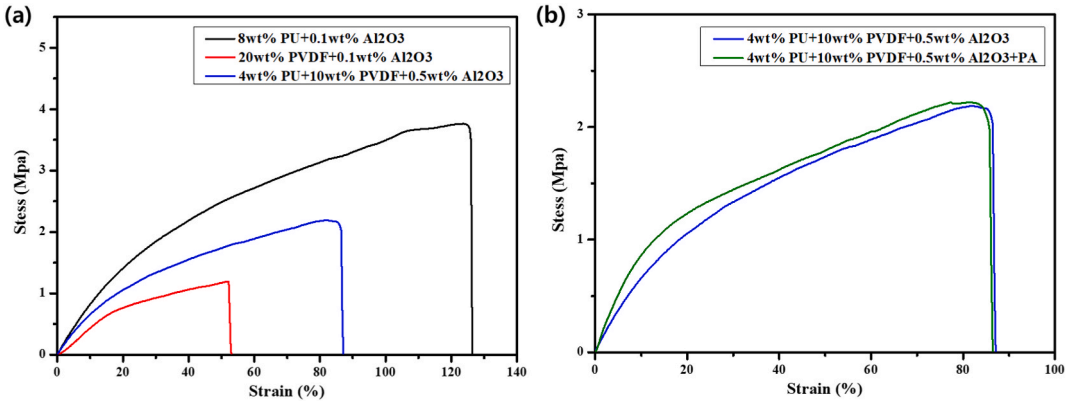

Fig. 6. Mechanical properties Test (a) PU/Al_2O_3 and PVDF/Al_2O_3 and PU/PVDF/Al_2O_3. (b) PU/PVDF/Al_2O_3 and PU/PVDF/Al_2O_3/PA.

oxide on Al foil appears when Al_2O_3 reacts with the carbon present in the polymer (Al–C state). Also, in the sample coated with Polyaniline on 4 wt% PU+10 wt% PVDF+0.5 wt% Al_2O_3 the peaks at 74.29 eV and 75.30 eV corresponding to Al were found (Fig. 4 (d)). In the case of 74.29 eV, it is the peak of Al oxide (Al state) and 75.30eV is the peak when the reaction with the carbon of the polymer occurs with Al oxide on Al foil as above (Al–C state). From the XPS spectrum, the presence of Al_2O_3 in both samples has been confirmed.

3.2. Thermogravimetric Analysis

Fig. 5 is the TG analysis tests conducted to evaluate the thermal stability of electrospun membranes. The thermal stability of PU at 280 and 374 °C corresponds to a loss of segments of urethane monomer bonds from the polymer chain on the first onset temperature, where almost 91% of the total weight of PU was lost (Fig. 5(a)). Beyond the 600 °C temperature, no remarkable change in weight loss occurred, which suggests the net weight of carbon remained as residual mass. The addition of Al_2O_3 along with the PVDF changes the onset temperature at 280 °C sharply indicating thermos-oxidative properties of PVDF suggesting the breakdown of C–F bonds (Fig. 5 (b)). However, the % of residual mass on the hybrid material is obviously higher than PU that confirm the higher wt % of carbon remaining at temp 900 °C (Fig. 5(c)).

3.3. Mechanical properties

The mechanical properties of the membrane were evaluated to utilize the prepared sample as a sensor (Fig. 6). As a sample for measuring the tensile strength, 8 wt% PU+0.1 wt% Al_2O_3 and 20 wt% PVDF+0.1 wt% Al_2O_3 and 4 wt% PU+10 wt% PVDF+0.5 wt% Al_2O_3 were compared. These samples are not as high in tensile strength as pure PU or pure PVDF because aluminum oxide nanoparticles are mixed. As the content of Al_2O_3 nanoparticles increases, these particles aggregate. The reason is that nanoparticles have a high surface area to volume fraction and high surface energy, making it difficult to uniformly disperse in a polymer nanofiber mat. It is also hydrophilic, so it is not compatible with a hydrophobic polymer nanofiber mat. Aggregated nanoparticles can act as stress concentration centers in the nanofiber mat and can adversely affect the mechanical properties of the nanofiber mat. Nevertheless, PVDF and Al_2O_3, which have better piezo and capacitance effects than PU, should be used. So, a small amount of PU was mixed with PVDF. As a result, it can be seen that the 4 wt% PU+10 wt% PVDF+0.5 wt% Al_2O_3 sample improved more than 2 times than the tensile

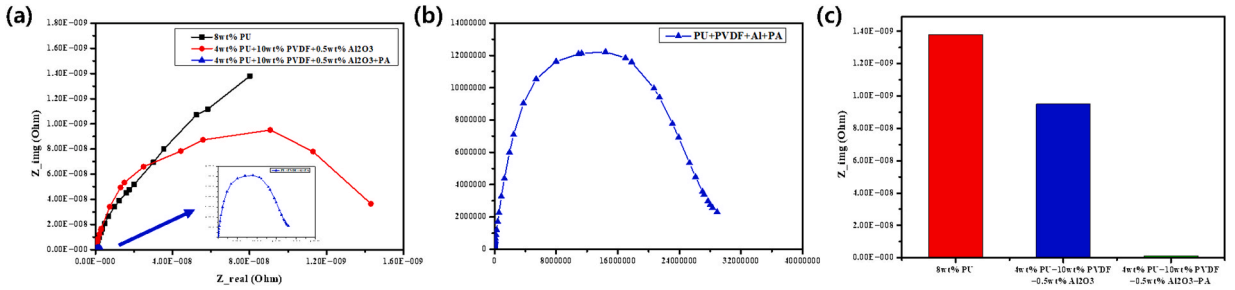

Fig. 7. Electrochemical test. (a) PU, PU+/PVDF/Al_2O_3 and PU/PVDF/Al_2O_3 +PA (b) graph of Z_img.

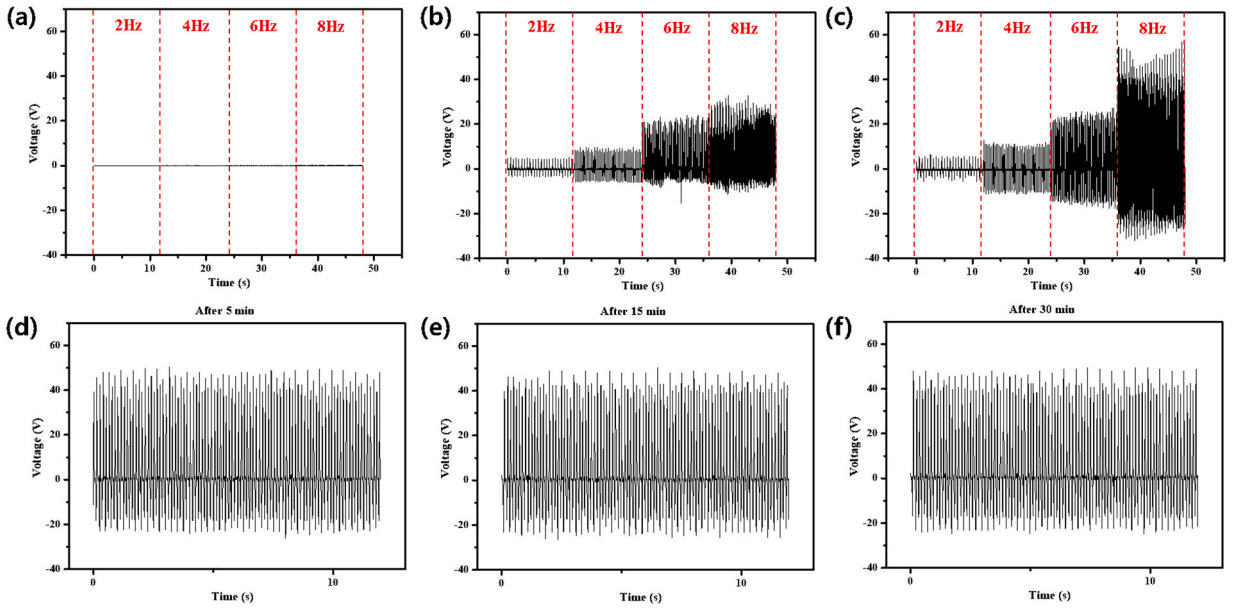

Fig. 8. Piezo Test of (a) PU, (b) PU/PVDF/0.1 wt% Al_2O_3, (c) PU/PVDF/0.5 wt% Al_2O_3, Long Time Test (d) 5 min, (e) 15 min, (f) 30 min.

strength of 20 wt% PVDF+0.1 wt% Al_2O_3 despite the content of the nanoparticles 5 times higher (Fig. 6(a)). In addition, the tensile strength of the sample coated with 4 wt% PU+10 wt% PVDF+0.5 wt% Al_2O_3 with Polyaniline was also measured. As a result, it can be seen that the coated sample has almost the same tensile strength when compared with the non-coated sample (Fig. 6(b)). And on the contrary, the initial coated sample is better. The tensile strength of the overall sample was decreased by mixing Al_2O_3 nanoparticles, but it was confirmed that the mechanical properties were better than 20 wt% PVDF+0.1 wt% Al_2O_3 by mixing PU to compensate.

3.4. Electrical properties

3.4.1. Electrochemical test

The EIS test, an electrochemical test, was conducted to confirm that the sensor has high capacitance when performing the LCR meter test (Fig. 7). We can compare the resistance of the sample through the EIS TEST. The formula for resistance can be expressed as:

$$R = \rho \frac{L}{A}$$

$$\rho = \frac{1}{\sigma}$$

$$R = \frac{L}{\sigma A}$$

σ is the electrical conductivity, ρ is the resistivity, R is the resistance, L is the length, and A is the area. It can be seen from this formula that resistance and conductivity are inversely proportional. In Fig. 7, the EIS TEST data can be found and compared. The five EIS tests per sample have been performed and the test result appeared in the shape of a semicircle as shown in Fig. 7. The larger the

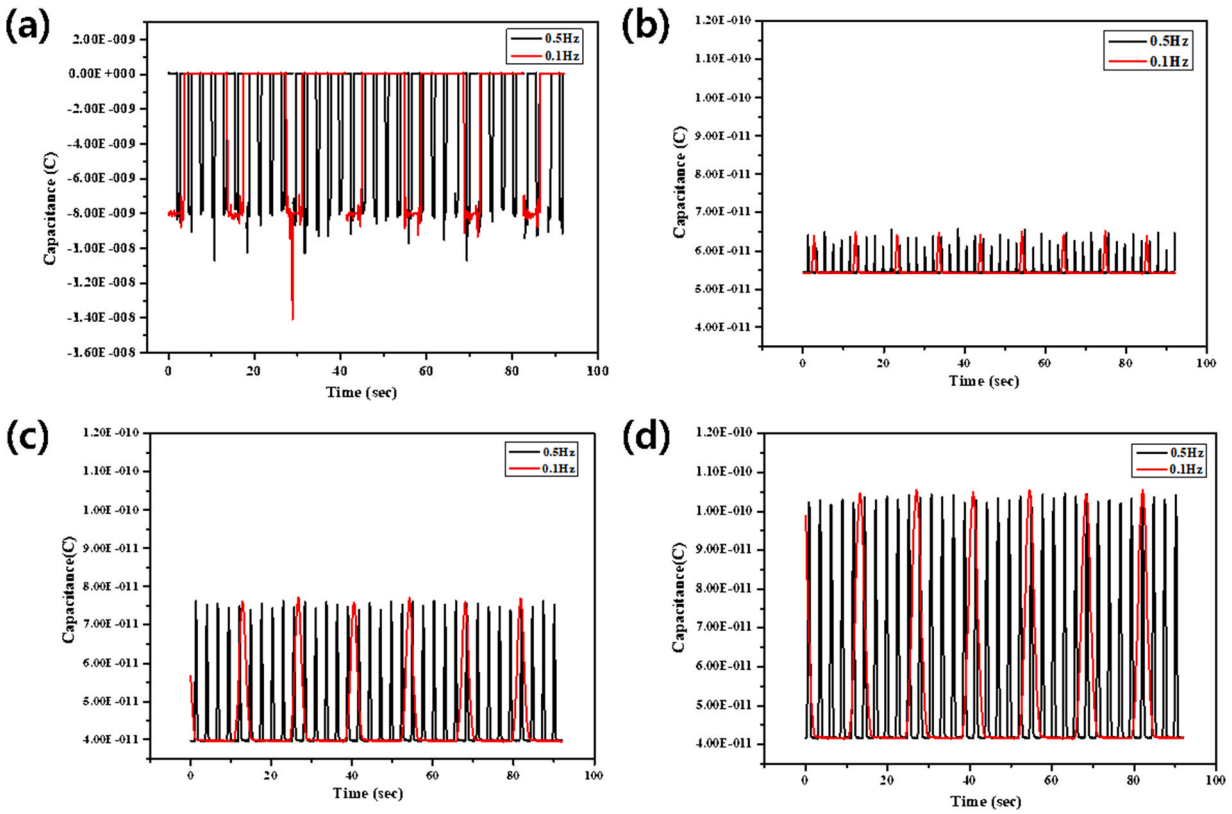

Fig. 9. LCR Meter Test of (a) PU, (b) PU/PVDF/0.1 wt% Al_2O_3, (c) PU/PVDF/0.5 wt% Al_2O_3, (d) PU/PVDF/0.5 wt% Al_2O_3/PA.

diameter of the circle, the greater the resistance. In 8 wt% PU, a complete semicircle did not appear, but it is possible to estimate the rest of the image with 50% of the image. In contrast, in the case of 4 wt% PU+10 wt% PVDF+0.5 wt% Al_2O_3 nanofibers, a semicircle having a diameter smaller than 8 wt% PU has been found. The data size of the sample coated with 4 wt% PU+10 wt% PVDF+0.5 wt% Al_2O_3 with Polyaniline is remarkably small (Fig. 7(a and b)). The maximum value of Z_img representing the radius of a semicircle is shown as a histogram in Fig. 7(c). 8 wt% PU has the largest resistance, 4 wt% PU+10 wt% PVDF+0.5 wt% Al_2O_3 has less resistance than 8 wt% PU, and 4 wt% PU+10 wt% PVDF+0.5 wt% Al_2O_3+Polyaniline sample has a small resistance. According to the above formula, 4 wt% PU+10 wt% PVDF+0.5 wt% Al_2O_3+Polyaniline is the largest, and 4 wt% PU+10 wt% PVDF+0.5 wt% Al_2O_3 is the second largest, and 8 wt% PU is the smallest. Since conductivity and capacitance are proportional, it can be proved that the 4 wt% PU+10 wt% PVDF+0.5 wt% Al_2O_3+Polyaniline coating sample has the largest capacitance in the LCR meter experiment.

3.4.2. Piezoelectricity

The sensor manufactured in this study is a self-powered sensor that does not require a separate battery, and a piezoelectric test was performed to confirm that it could generate a voltage on its own (Fig. 8). When checking the piezoelectric test results of each sample group, it was confirmed that the electrospun pure PU membrane had a small piezoelectric effect (Fig. 8(a)). In addition, when PVDF and Al_2O_3 were added, the voltage was generated when stimulation was given, and it was confirmed that as each content increased, the generated voltage also increased (Fig. 8(b and c)). In addition, when the sensor is applied to the actual human body, it must have the ability to detect human body signals for a long time. To test this, a piezoelectric test was conducted for more than 30 min, and the change in piezoelectric performance over time was measured (Fig. 8(d ~ f)). As a result of checking the voltage value generated when stimulation was applied for (5, 15, and 30) min, it was confirmed that there were no problems, such as a greatly changing piezoelectric value, or damage to the sensor over time. Through this, it is expected that when applied to actual patients, the sensor manufactured in this study can be used for a long time.

3.4.3. Sensitivity

To check whether the sensor manufactured in this study could detect the electrical signal of the patient's body, an LCR meter test was conducted (Fig. 9). Analyzing each measurement result, first, in the case of the electrospun PU sample, when pressure was applied, the capacitance was measured as a negative number below zero (Fig. 9(a)). This means that the signal applied to the sensor could not be measured, because it had almost no electrical conductivity. Comparison of Fig. 9(b) and (c) using the same ratio of PU and PVDF and varying the ratio of Al_2O_3 shows that the higher the ratio of Al_2O_3, the higher the electrical conductivity. In addition, (d) with polyaniline coating on (c) confirmed 25 % improved capacitance, compared to (c). Through this, it was also confirmed that the polyaniline

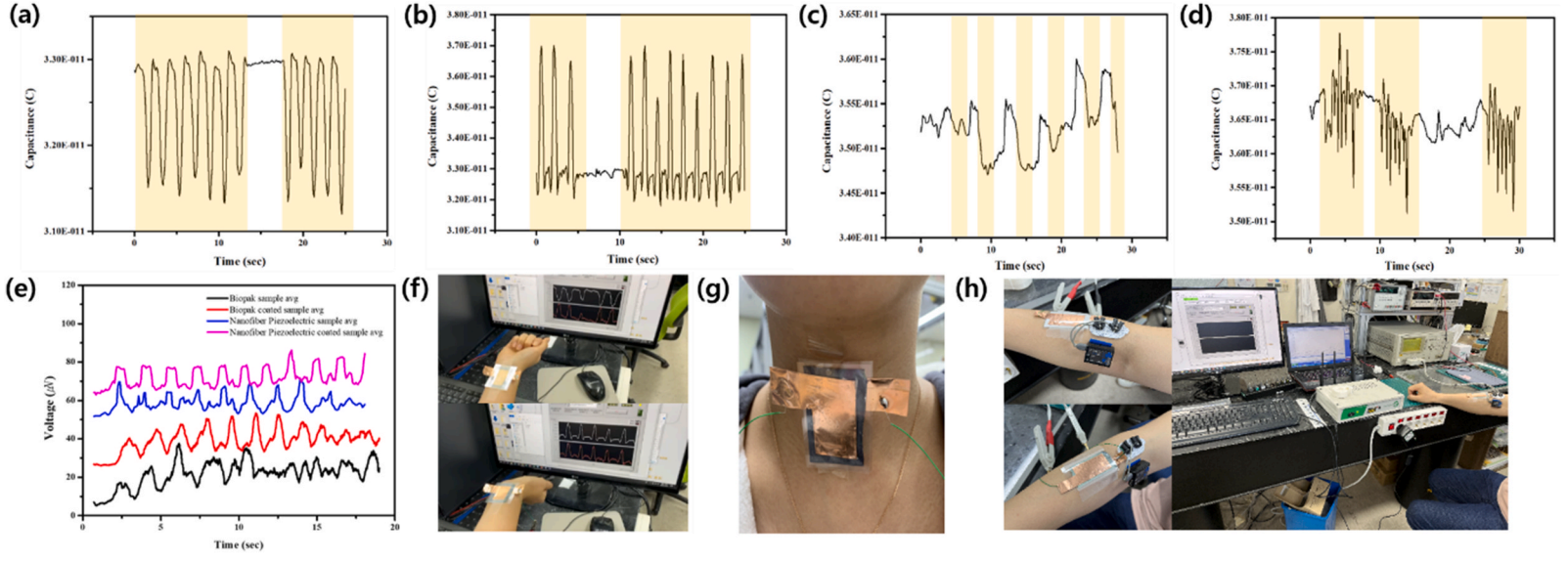

Fig. 10. Sensor Sensitivity Test (a) Bending, (b) Stretching, (c) discontinuous voice, (d) continuous voice, (e) EMG Test (*vs.* BioPac), Sensor attached on (f) Wrist, (g) neck and (h) arm.

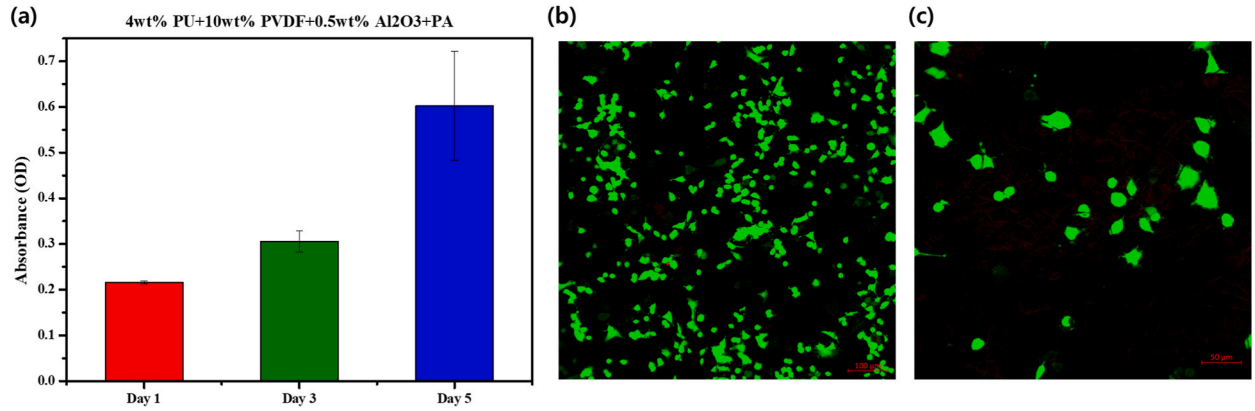

Fig. 11. (a) In Vitro Cell Counting Test, (b) and (c) Confocal Image (Live and dead).

coating improved the electrical conductivity of the sample. Each conductive material used in this study was added, and the higher the ratio, the higher the capacitance, which indicates high detectability for electrical signals. Therefore, it was confirmed that sample (d) showing the highest capacitance was the optimal sensor to detect the patient's signal.

Using sample (d), which showed the highest detection efficiency in Fig. 9, an experiment was conducted to detect signals from an actual human body. The prepared sensors were attached to the wrist and neck, respectively, and the experiment was conducted using an LCR meter (Fig. 10). As a result of attaching the sensor to the skin and moving the wrist (Fig. 10(f)), it was confirmed that the capacitance value changed as shown in the graph according to the movement of the wrist (Fig. 10(a and b)). Next, a sensor was attached to the neck to see if it could detect voice vibrations that occur when speaking. As a result of the check, as can be seen in Fig. 10 (c and d), the attached sensor confirmed each capacitance change by changing the graph according to the discontinuous and continuous sound.

In addition, experiments were conducted to compare the developed sensor with currently commercialized sensor products. As a sensor that is actually commercialized, the BIOPAC system (Bioresearch Inc, USA) used for electromyography was used, and a comparative experiment was conducted by preparing samples according to the presence or absence of PA coating. The BIOPAC and this experimental sensor were attached to the arm at the same time (Fig. 10(h)), and the movement of the muscles was measured by repeating the motion of forming and releasing a fist. Fig. 10(e) shows that the developed sensor detects muscle movement simultaneously with the BIOPAC electromyograph. In order to test the sensors simultaneously, the measurement was performed after placing the sensors at regular intervals as shown in the figure, so there was a slight error in the result, but the detection accuracy was almost the same. Through this experiment, it was confirmed that the sensor developed through this study showed similar results to BIOPAC used for electromyography, and it was proved that when applied in actual clinical practice, it could detect the patient's physical and electrical signals.

3.5. In vitro cell study

The sensor must be attached to the body in order to detect signals from the human body. If necessary, it can be used inside the human body. Accordingly, the biocompatibility of the sensor was evaluated (Fig. 11). Using PC12 cells, after releasing the cells, it was first evaluated how many cells were grown. After 1, 3, and 5 days, the number of cells was checked. The number of cells increased from day 1 to day 3. From day 3 to day 5, the number of cells also increased (Fig. 11(a)). It was confirmed that the sample was under conditions in which cells could grow well. In addition, after culturing the cells, it was confirmed how many cells were alive using Confocal. Using dye, living cells appear green and dead cells appear red. In the confocal image, living green cells can be identified, and dead red cells cannot be identified (Fig. 11(b and c)). As a result, it was confirmed that this sensor is biocompatible because cells can grow well and are harmless to the human body.

4. Conclusion

In this study, a new method of developing a biosensor that can detect physical and electrical signals, such as the patient's voice and electromyogram, was presented. To increase the sensitivity indicating the accuracy of the sensor, a mixture of PU and PVDF, a conductive polymer, was used. In addition, after adding the conductive material Al_2O_3, it was manufactured into a membrane through electrospinning. In addition, the prepared membrane was coated with polyaniline, a conductive polymer. It displayed high piezoelectric performance through the piezo experiment, and it was confirmed through the LCR meter test that it has high sensitivity. In addition, when the experiment was conducted after being attached to the actual human body, it was confirmed that the measurement of the body reaction was possible. The sensor made through this study has piezoelectric performance capable of self-charging and discharging and can detect sound and movement signals with high sensitivity based on high conductivity. In addition, it has biocompatibility, can actually be attached to the patient's skin, and can sense the physical and electrical signals of the body. When

using the sensor developed in this study, it is expected that their health condition can readily be detected by sensing the patient's daily activities in daily life.

Data availability

All data generated or analyzed during this study are included in this published article.

CRediT authorship contribution statement

Eun Ae Choi: Conceptualization, Data curation, Formal analysis, Investigation, Methodology, Writing – original draft, Writing – review & editing. **Jeong Chan Lee:** Data curation, Writing – review & editing. **Mi Yu:** Data curation, Methodology. **Hyo Sung Kwak:** Supervision, Validation. **Bishnu Kumar Shrestha:** Conceptualization, Methodology, Supervision, Validation, Writing – original draft. **Chan Hee Park:** Supervision, Funding acquisition. **Cheol Sang Kim:** Supervision.

Declaration of competing interest

The authors declare that they have no known competing financial interests or personal relationships that could have appeared to influence the work reported in this paper.

Acknowledgement

This work was supported by the Korea Medical Device Development Fund grant funded by the Korea government (the Ministry of Science and ICT, the Ministry of Trade, Industry and Energy, the Ministry of Health & Welfare, Republic of Korea, the Ministry of Food and Drug Safety) (1711195494, RS-2020-KD000005).

This work was supported by the material parts technology development Program (20017672, Development of manufacturing technology for electromagnetic shielding and heat dissipation composite material based on eco-friendly two-component mixed electrospinning technology) funded By the Ministry of Trade, Industry & Energy (MOTIE, Korea).

This paper was supported by Fund of Biomedical Research Institute, Jeonbuk National University Hospital.

References

[1] D. Lu, Y. Yan, Y. Deng, Q. Yang, J. Zhao, M.H. Seo, W. Bai, M.R. MacEwan, Y. Huang, W.Z. Ray, J.A. Rogers, Adv. Funct. Mater. 30 (2020).
[2] Y. Zhang, H. Xiao, IEEE Trans. Inf. Technol. Biomed. 13 (2009) 1040–1048.
[3] P.S. Pandian, K.P. Safeer, P. Gupta, D.T. Shakunthala, B.S. Sundersheshu, V.C. Padaki, J. Network. 3 (2008).
[4] J. Li, Y. Long, F. Yang, H. Wei, Z. Zhang, Y. Wang, J. Wang, C. Li, C. Carlos, Y. Dong, Y. Wu, W. Cai, X. Wang, Adv. Funct. Mater. 30 (2020).
[5] K. Lee, X. Ni, J.Y. Lee, H. Arafa, D.J. Pe, S. Xu, R. Avila, M. Irie, J.H. Lee, R.L. Easterlin, D.H. Kim, H.U. Chung, O.O. Olabisi, S. Getaneh, E. Chung, M. Hill, J. Bell, H. Jang, C. Liu, J.B. Park, J. Kim, S.B. Kim, S. Mehta, M. Pharr, A. Tzavelis, J.T. Reeder, I. Huang, Y. Deng, Z. Xie, C.R. Davies, Y. Huang, J.A. Rogers, Nat. Biomed. Eng. 4 (2020) 148–158.
[6] C. Lang, J. Fang, H. Shao, X. Ding, T. Lin, Nat. Commun. 7 (2016) 11108.
[7] S.K. Ghosh, D. Mandal, Appl. Phys. Lett. 110 (2017).
[8] N. Shehata, A.H. Hassanin, E. Elnabawy, R. Nair, S.A. Bhat, I. Kandas, Sensors (2020) 20.
[9] W. Wang, P.N. Stipp, K. Ouaras, S. Fathi, Y.Y.S. Huang, Small 16 (2020) e2000581.
[10] Z. Zhan, R. Lin, V.T. Tran, J. An, Y. Wei, H. Du, T. Tran, W. Lu, ACS Appl. Mater. Interfaces 9 (2017) 37921–37928.
[11] X. Chen, S. Guo, J. Li, G. Zhang, M. Lu, Y. Shi, Sensor Actuator Phys. 199 (2013) 372–378.
[12] X. Li, W. Chen, Q. Qian, H. Huang, Y. Chen, Z. Wang, Q. Chen, J. Yang, J. Li, Y.W. Mai, Adv. Energy Mater. 11 (2020).